The effect of CaO to MgO ratio on the smelting characteristics of vanadium-bearing titaniferous magnetite

M. Sitefane, M. Masipa, P. Maphutha, and X.C. Goso

Mintek, Randburg

Laboratory-scale test work was conducted to study the effect of the CaO to MgO ratio on the carbothermic smelting of titaniferous magnetite (titanomagnetite) for the recovery of titanium. The smelting characteristics were studied using the original limestone-dolomite fluxing strategy with a CaO to MgO ratio of 22:8 and the updated dolomite fluxing strategy with a CaO to MgO ratio of 16:14 applied on a commercial scale by Evraz Highveld Steel and Vanadium (EHSV). These fluxing strategies result in similar liquidus temperatures. The smelting test work results revealed that Fe and V recoveries to the alloy phase were similar for both fluxing strategies and were also comparable to that observed in the EHSV process. However, the titanomagnetite slag with a target CaO:MgO ratio of 22:8 had a significant content of perovskite, pseudobrookite, and spinel phases. The dominance of perovskite and pseudobrookite in the slag shows that titanium reports mainly to these two phases, presenting an opportunity for further beneficiation of the titanomagnetite slag. Titanium is recovered from ilmenite slags containing primary pseudobrookite phases by leaching or chlorination. It is also recoverable from a perovskite phase by a salt roast followed by a double water-acid leach process.

INTRODUCTION

Vanadium-bearing titaniferous magnetite (titanomagnetite) deposits offer the unprecedented opportunity of deriving three saleable products from the same resource, namely iron, vanadium, and titanium. In South Africa, vanadiferous titanomagnetite is found mainly in the upper zone of the Bushveld Complex (Fischer, 1975). In the past, the use of conventional blast furnace technology for smelting the Bushveld and similar high-titanium titanomagnetite ores was deemed unfeasible owing to the possible formation of high-melting reduced titanium species that would require a higher coke rate and would descend into the cohesive zone as unmelted solids. In 1949, Dr William Bleloch successfully demonstrated an innovative process for the smelting of the Bushveld titanomagnetite containing about 13% TiO_2 using a submerged arc furnace. The innovative process involved the smelting of titanomagnetite in the presence of a carbonaceous reductant and a flux to produce a valuable vanadium-bearing pig iron and an essentially valueless low titania (TiO_2) slag containing about 35% TiO_2 (Bleloch, 1949).

In 1961, the submerged arc furnace technology was implemented by the Highveld Development Company, known today as Evraz Highveld Steel and Vanadium Corporation (EHSV), to process their titanomagnetite ore mined from Mapoch mine in a submerged arc pilot plant furnace to produce 10 t of pig iron per day. The pig iron was further processed to produce vanadium and steel products, while the titania-bearing slag was discarded as waste (Rohrmann, 1985). The EHSV pilot operation was commissioned with a flux mixture of limestone, dolomite, and quartz in a ratio of 21:20:6 to target a slag with CaO and MgO contents of 22% and 8%, respectively (Jochens *et al*., 1969).

During the development of the EHSV operation, dolomite was relatively cheap and readily available in the Northern Transvaal (now Gauteng) compared to limestone. In 1969, Jochens *et al*. conducted a comprehensive study to gather information on the possibility of replacing all the limestone in the smelting flux by dolomite, *i.e.* to target a slag with CaO and MgO concentrations of 16% and 14%, respectively. The scope of the test work involved the establishment of more information regarding the equilibrium and non-equilibrium behaviour of titanomagnetite slags, with particular reference to the MgO to CaO ratio. The phase equilibrium diagram shown in Figure 1 was established as part of the research. As illustrated by the dashed line on the phase diagram, it transpired that the dolomite flux would result in a slight lower liquidus temperature of 1375°C compared to the 1390°C in the limestone/dolomite flux. Although it was proven that the smelting process could be successful with the use of dolomite only as flux, instead of dolomite and limestone, there was also a shift in the slag primary phase from perovskite ($CaTiO_3$) to a pseudobrookite-type solid solution $4(MgO.2TiO_2).Al_2O_3TiO_2$ (Jochens *et al*., 1969).

Titania is recoverable from ilmenite slags containing a primary pseudobrookite phase through various process routes, including the Upgraded Slag (UGS) process (van Dyk, 1999). A study by Zhang *et al*. (2007) revealed the feasibility of recovering titania from titanomagnetite slags that contain perovskite, *i.e*., the original EHSV titanomagnetite slag before the change in fluxing strategy. The titania recovery process involves the growing of the perovskite phase by concentrating most of the titania in the slag into this phase under dynamic oxidation conditions. The perovskite phase is typically extracted from the slag by flotation (Zhang *et al*., 2007). Titania is then recovered from the perovskite phase by a salt roast and double water-acid leach process (Wang *et al*., 2010).

The study by Jochens *et al*. (1969) dealt with the economic intensification of the titanomagnetite smelting process in terms of operational temperatures and monetary savings on the flux, while the steel and vanadium recoveries were still in the acceptable range and the titania-bearing slag was stored on a slag dump. The shift in primary phase therefore did not deter the resolution of replacing all limestone in the flux by dolomite and the titanomagnetite by titania-bearing slag accumulated at EHSV over the years to more than 40 Mt (Anderson, 2013). A notable impact of the phase shifts was the subsequent complication of the slag phase chemistry such that the slag cannot be treated further by the available titania slag upgrading processes. Of further interest is that the analysis of the EHSV slag showed the presence of spinel in the slag, which is not predicted by Jochens' phase diagram. The analysis showed that either the spinel or the pseudobrookite could have crystallized as a primary phase (Goso *et al*., 2015).

The current study was initiated to investigate the effect of the shift between limestone-dolomite and dolomite fluxing strategies, *i.e*. the ratio of CaO to MgO, on the smelting characteristics of titanomagnetite. Vanadium and iron recoveries were reviewed when operating with slags containing perovskite and pseudobrookite primary phases with a view of recovering titania from the titanomagnetite slag.

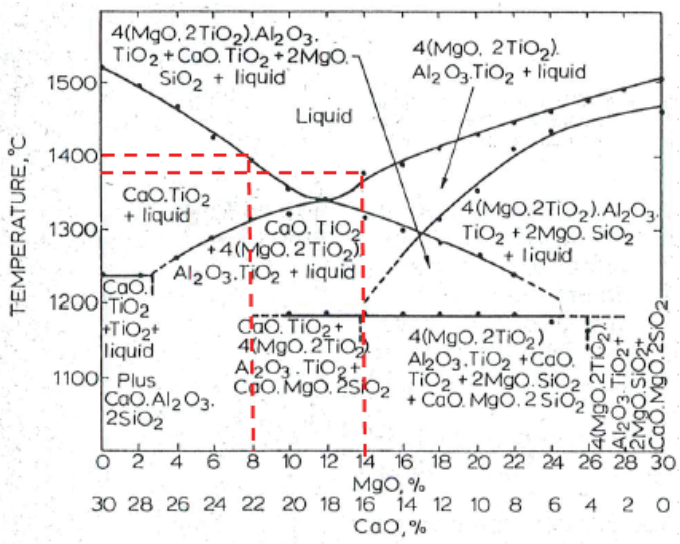

Figure 1. Phase equilibrium diagram for the slag system 19.69% SiO_2, 13.12% Al_2O_3, 37.19% TiO_2, 30% (CaO + MgO), the latter being varied from 30% CaO and 0% MgO to 0% CaO and 30% MgO (Jochens *et al.*, 1969)

EXPERIMENTAL

Materials

The laboratory scale test work was undertaken using a titanomagnetite material supplied by EHSV. The sourcing of the titanomagnetite material from EHSV was strategic for this test work in order to allow for the comparison of the results to the EHSV plant data. The bulk chemical compositions of the feed titanomagnetite material to the EHSV process and for the current test work were obtained from Steinberg *et al.* (2011) and analysis at Mintek, respectively. The chemical compositions of these feed materials are given in Table I. The two feed samples are very similar, suggesting that they originated from the same reserve. The chemical composition of the feed sample for the current test work is also reported in elemental form in order to allow for the evaluation of the elemental deportment after smelting.

Synthetic fluxes were made by combining high-purity MgO, Al_2O_3, SiO_2, and CaO from Associated Chemical Enterprises (ACE). The carbonaceous reductant was a low-sulphur carbon (Sascarb) from Sasol. The typical compositions of the synthetic fluxes and reductant are given in Table II. High-purity alumina crucibles from Kayla Africa Suppliers and Distributors were used.

The bulk chemical compositions of feed and product samples were determined by inductively coupled plasma–optical emission spectrometer (ICP–OES) using a Varian Vista-PRO instrument. The total carbon and sulphur concentrations of alloy products were determined using CS–230 and CS-744 LECO instruments. The morphological and phase chemical compositions of the slag products were determined by scanning electron microscopy (SEM) using energy dispersive spectrometry (EDS) (Zeiss MA15 equipped with a Bruker energy dispersive spectrometer) and X-ray diffractometry (XRD) (Bruker D8 Advance X-ray diffractometer), respectively.

Table I. Chemical compositions of the feed titanomagnetite materials (mass%).

	Fe_3O_4	MgO	Al_2O_3	SiO_2	CaO	TiO_2	V_2O_5	Cr_2O_3	MnO
Mintek tests	77.71	1.48	3.97	1.34	0.07	13.31	1.67	0.20	0.24
EHSV operation	76.5	1.60	4.80	2.00	0.10	12.7	1.65	0.40	0.30
	Fe	Mg	Al	Si	Ca	Ti	V	Cr	Mn
Mintek tests	56.23	0.89	2.10	0.63	0.05	7.97	0.93	0.14	0.19

Table II. Composition of the reductant and synthetic fluxes (mass%).

	C	MgO	Al_2O_3	SiO_2	CaO	Ash	Loss on ignition
MgO		99.0					
Al_2O_3			98.0				
SiO_2				98.5			
CaO					96.0		3.50
Sascarb	98.7					0.33	0.97

Smelting Recipe Preparation

The smelting recipes were prepared to target two slag compositions, namely limestone-dolomite fluxing (CaO = 22% and MgO = 8%) and dolomite-only (CaO = 16% and MgO = 14%) slags. In order to be able to reference Jochens' phase diagram (Jochens *et al.*, 1969), the concentrations of SiO_2 and Al_2O_3 in the smelting recipes and the overall flux mass (for TiO_2 dilution) were adjusted such that the compositions of the subsequent slags were similar to those defined in the reference phase diagram – SiO_2 =19.69%, Al_2O_3 = 13.12%, and TiO_2 = 37.19%. The SiO_2 and Al_2O_3 additions as well as the overall flux mass were kept constant in the test recipes, with adjustments to the CaO to MgO ratio to maintain a total mass of 30 g (CaO + MgO). The reductant addition was studied as the main parameter in each of the slag compositions. The Sascarb addition was varied between 90% and 120% by mass of the stoichiometric requirement for the reduction of iron and vanadium in the titanomagnetite feed. The chemical reactions shown in Equation [1] and [2] were used for the calculation of the reductant carbon requirements. The smelting test recipes were mixed as summarized in Table III.

$$Fe_3O_4 + 4C \rightarrow 3Fe + 4CO \quad [1]$$

$$V_2O_5 + 5C \rightarrow 2V + 5CO \quad [2]$$

The respective recipes were prepared by weighing and mixing the components in a clean plastic container. Each mixture was transferred into the milling jar of a ring mill and milled for 30 seconds to homogenize it. The homogenized material was weighed and densely packed in a high-purity alumina crucible.

Table III. Target CaO:MgO ratios, reductant additions, and normalized smelting test recipes (normalized to a total of 100 g)

Test	CaO:MgO	Reductant (% of stoichiometric)	Titanomagnetite	Al_2O_3	CaO	MgO	SiO_2	Sascarb
1	22:8	90	76.60	0.58	6.23	1.07	4.45	11.07
2	22:8	100	75.67	0.57	6.15	1.06	4.39	12.16
3	22:8	110	74.76	0.56	6.08	1.05	4.34	13.21
4	22:8	120	73.87	0.56	6.01	1.04	4.29	14.24
5	16:14	90	76.65	0.58	4.52	2.73	4.45	11.08
6	16:14	100	75.71	0.57	4.46	2.70	4.39	12.16
7	16:14	110	74.80	0.56	4.41	2.67	4.34	13.21
8	16:14	120	73.91	0.56	4.36	2.64	4.29	14.24

Smelting

A 30 kW induction furnace was used. A schematic set-up of the induction furnace is shown in Figure 2. Crucibles containing samples were heated inside a graphite susceptor. The smelting tests were conducted in four sets of two tests (eight tests in total). The smelting test procedure entailed placing two charged crucibles in the induction furnace chamber, comprising the a graphite susceptor with the base covered with high-purity alumina bubbles. The graphite susceptor was closed with a lid that had

three holes: the first for an alumina sheath containing a B-type thermocouple used to monitor sample temperature, the second for an open-ended alumina sheath to supply argon gas to create an inert atmosphere inside the susceptor, and the last to vent off-gas. The induction chamber was insulated by alumina bubbles, taking care to prevent the bubbles from entering the test crucibles. An additional insulation layer was provided by an alumina-silicate based ceramic blanket (Fibrefrax®). The thermocouple was connected to a data logging system and the argon cylinder was opened to allow a continuous flow of argon for the duration of the test.

Samples were heated inside the furnace from room temperature at a rate 10°C/min up to the reaction temperature of 1600°C. Once at temperature, the power was adjusted such that the temperature could be maintained at the reaction temperature for 1 hour. The holding temperature was in the order of 200°C above the liquidus temperature of the slag in order to reduce the slag viscosity and maximize separation between the slag and the alloy phases. After 1 hour, the furnace power was switched off and the samples were allowed to cool overnight to room temperature in an argon atmosphere with a consistent flow of argon gas and cooling water. The cold test crucibles were removed from the furnace, weighed, and broken to recover the alloy and slag. The alloy button was weighed and the mass of the slag calculated by difference. In a few cases the alloy was collected as globules and subsequently mixed with the alloy button to estimate the total mass of the alloy. Clean alloy and slag samples were collected and submitted for bulk chemical characterization by ICP-OES and LECO. The clean slag samples were further analysed using SEM-EDS and XRD.

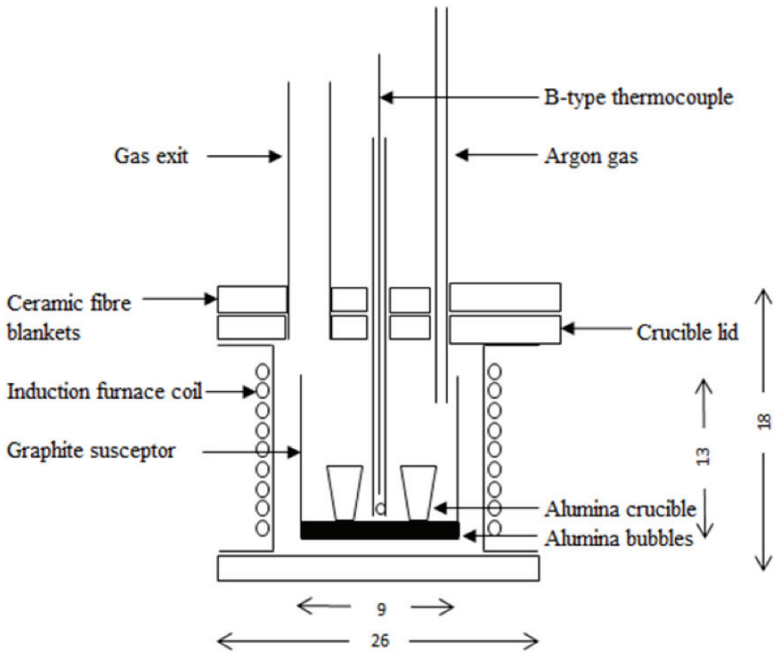

Figure 2. Schematic diagram of the 30 kW induction furnace (dimensions in cm).

RESULTS AND DISCUSSION

Smelting Product Masses

A photograph illustrating the general appearance of smelting test products is shown in Figure 3. The photograph shows that there was generally a good separation between the slag and the alloy, with little or no entrainment of the alloy within the slag phase. For analysis purposes, samples were collected from the unmixed parts of the slags and alloys.

The masses of the smelting test products are summarized in Table IV. The major source of mass loss in the smelting tests was the carbon monoxide (CO) produced during the reduction of magnetite and vanadium oxide as shown in Equations [1] and [2]. The slag mass percentages indicate the amount of the solid material that did not collect to the alloy after smelting. The alloy mass percentages (alloy fall mass%) signify the amount of the smelter feed that collected at the base of crucible to form an alloy button. In few cases the alloy was collected as globules and subsequently mixed with the alloy button to estimate the total alloy fall.

To study the effect of reductant addition, the mass% metal produced was plotted as a function of the stoichiometric reductant addition (see Figure 4). For both slag recipes, the best metal yields were achieved with 100% stoichiometric reductant addition. At 100% stoichiometric reductant addition, slightly more metal formed with the original slag system (a CaO:MgO ratio of 22:8 *vs.* 16:14). At reductant additions above stoichiometric requirements, the metal yield was significantly less – this was attributed to reduced slag-metal separation due to an increase in melt viscosity and the dilution effect of solid unreacted carbon present in the system.

Figure 3. General appearance of the smelting test products

Table IV. Smelting product relative masses (mass%)

Test	CaO:MgO	Reductant (% of stoichiometric)	Loss	Slag	Alloy	Total
1	22:8	90	39.1	19.4	41.5	100
2	22:8	100	20.3	30.4	49.3	100
3	22:8	110	30.4	30.4	39.2	100
4	22:8	120	31.5	40.9	27.6	100
5	16:14	90	29.3	27.9	42.8	100
6	16:14	100	30.2	27.0	42.8	100
7	16:14	110	30.6	28.3	41.2	100
8	16:14	120	31.2	49.6	19.2	100

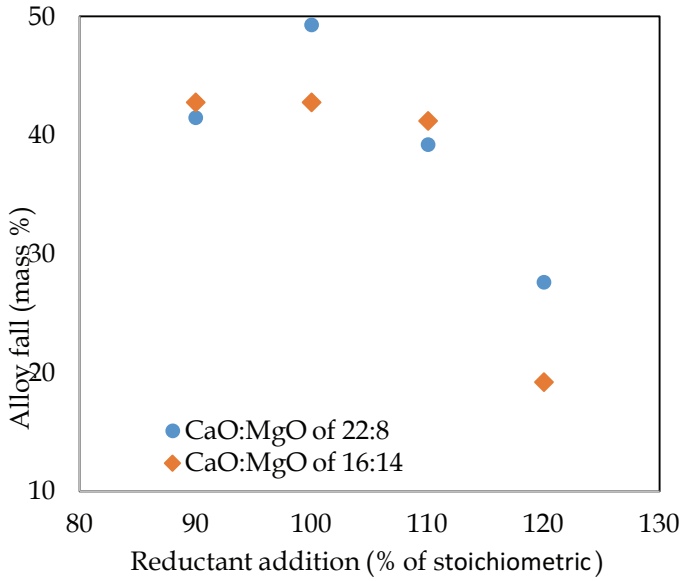

Figure 4. The relationship between the alloy fall and the reductant addition ('stoichiometric reductant addition' refers to the amount of carbon required. '100%' refers to the amount required to reduce all iron and vanadium oxide to alloy form)

Alloy Characteristics

The alloy produced in the titanomagnetite smelting operation should be compatible in terms of liquidus temperature (a function of carbon content in the alloy) for the recovery of the vanadium as vanadium slag and the production of steel in the downstream processes. The chemical compositions of the alloys produced in the experiments and that of the typical alloy produced by EHSV are given in Table V. The results show that the concentrations of Ti and C in the alloy increase with increasing reductant addition for both slag systems. At EHSV the Ti and C concentrations in the alloy were used as an indicator in the furnace chemistry control system. The term 'chemistry satisfactory' was used to confirm that the alloy had the desired grade. The desired grade referred to an alloy with a C content of 3.5%, V content of 1.2%, and Ti content of about 0.18%. The EHSV alloy chemical composition is generally similar to the chemical compositions of the eight alloys produced in the current test work, except for the alloys produced at higher carbon additions (110% and 120% of stoichiometric), which reported higher Ti concentrations than the specification. The high Ti in the alloy indicates a highly reducing environment. In the EHSV operation, the high Ti content in the alloy meant that other residual elements in the alloy were also high, thus consuming more energy. The problem was dealt with by increasing the feed rates of a correction material to dilute the reducing conditions and control the furnace energy input (Steinberg, dspace, 2008).

The recoveries of Fe and V to the alloy phase (as calculated by Equation [3]) were plotted as a function of reductant addition as shown in Figure 5. The recoveries of Fe and V at EHSV were deduced from data in literature to be about 95% and 77% respectively (Steinberg, dspace, 2008). The results of the current test work show that the recoveries of Fe and V to the alloy with carbon additions of 90% and 100% stoichiometric are comparable to the commercial plant recoveries. When the conditions became highly reducing, the alloy fall and Fe and V recoveries decreased, possibly due to alloy entrainment in the slag. The best and the worst Fe and V recoveries to alloy were achieved when smelting was conducted with a target CaO:MgO ratio of 22:8 in the slag. This may indicate that this slag system is more sensitive to variation in carbon reductant addition than the updated EHSV slag system with a CaO:MgO ratio of 16:14. Other than that, there is no significant difference in the characteristics of the alloy produced at the targeted CaO:MgO ratios of 22:8 and 16:14. The high (>100%) recoveries of Fe in a slag with target CaO:MgO ratio of 22:8 were attributed to measurement uncertainty.

$$\text{Recovery of element } i \text{ to alloy} = \frac{\text{mass of element } i \text{ in alloy}}{\text{mess of element } i \text{ in feed}} \times 100 \quad [3]$$

Table V. Chemical compositions of the alloys (mass%)

Test	Al	Si	Ti	V	Cr	Mn	Fe	Ni	C	Total
EHSV alloy	-	0.20	0.20	1.29	0.34	-	94.5	-	3.20	99.7
1	0.19	<0.025	0.12	1.29	0.42	0.04	93.7	0.04	1.36	95.8
2	0.19	0.33	0.24	1.36	0.40	0.11	94.6	0.11	1.40	97.3
3	0.29	0.45	0.54	1.40	0.40	0.14	92.6	0.14	1.33	96.0
4	0.21	0.39	0.89	1.33	0.42	0.17	91.6	0.17	1.29	95.2
5	0.10	<0.025	0.04	0.86	0.32	0.04	94.8	0.13	1.30	96.3
6	0.09	0.09	0.08	1.30	0.41	0.07	93.2	0.11	1.32	95.3
7	0.15	0.45	0.42	1.33	0.42	0.15	94.4	0.12	1.38	97.4
8	0.17	0.36	0.68	1.38	0.46	0.18	93.8	0.12	0.84	97.1

Mg, Ca, and Cu <0.005%: respective analyte concentrations are below the detection limit
<0.025%: analyte concentration is below the detection limit. - Not reported

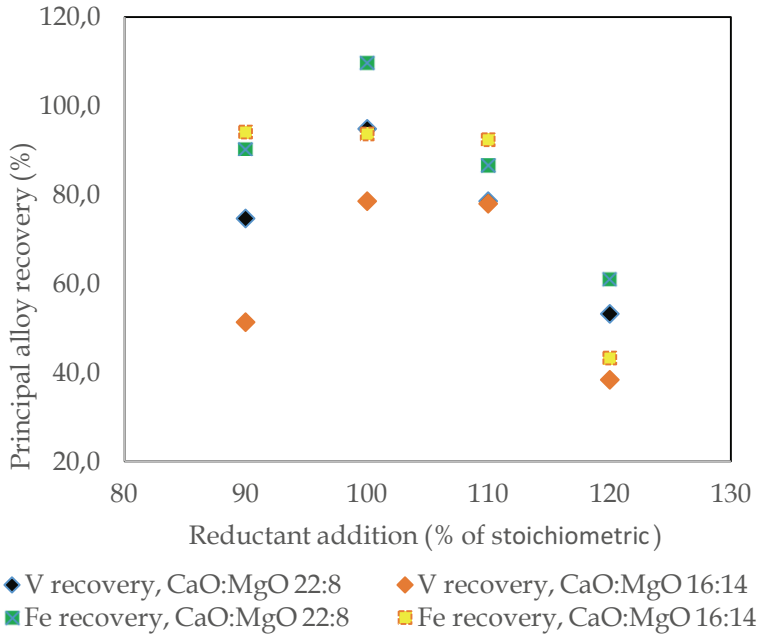

Figure 5. The relationship between the Fe and V recoveries to alloy and the reductant addition (recoveries above 100% are possibly due to a dilution effect)

Slag Characteristics

Titanomagnetite slags generally do not have direct economic importance in the titanomagnetite smelting operations as they are not processed further. However, a fundamental understanding of titanomagnetite slag characteristics is very important because the slag certainly has an effect on the furnace operation, vanadium and iron recoveries thus contributing to the costs of the operation. Furthermore, slag disposal on a waste dump adds to the cost of the operation, and remains an environmental liability even when production ceases. As recovery of titania from the slag is a potential solution to the problem, the testwork results, as a means of evaluating possible titania recovery, are presented below in two sections: chemical and mineralogical analysis.

Chemical Analysis

The bulk chemical compositions of the slags produced from the current test work and that of EHSV slag are given in Table VI. The chemical composition of the plant slag is different to the slags produced in the current test work. The slags produced in Test 5 to Test 8 were anticipated to be very close in composition to the plant slag because a similar fluxing strategy was used – in the test work a synthetic dolomite flux was used and in the EHSV plant operation, natural dolomite is used. The reason for the major difference in the slag chemical compositions is contamination of the slag by Al_2O_3 as a consequence of crucible wear. In the case of the slag with a target CaO:MgO ratio of 22:8, the alumina contamination was more severe – this suggests that this slag was more corrosive towards the alumina crucible. Evaluation of the CaO-MgO-Al_2O_3 ratio proved this, as higher CaO/MgO ratios can take up slightly more alumina than the lower CaO/MgO before saturation. The effect of crucible wear on titanomagnetite slags is a subject of another project at Mintek. In all the cases, the crucible wear resulted in significant dilution of the slags; hence the target concentrations of CaO, MgO, TiO_2, Al_2O_3, and SiO_2 were not met. In particular, the TiO_2 grades in the slags produced with a target CaO:MgO ratio of 22:8 were very low.

In most instances, the primary indicator of the efficiency of the recovery of valuable commodities is the amount of these commodities in the byproduct stream. It should be noted that the concentrations of Fe and V in the slag were also diluted by alumina from erosion of the crucible. Nevertheless, as shown in Table VI, the by-product slags with the lowest amounts of FeO and V_2O_5 in both slag systems, *i.e.* with target CaO:MgO ratios of 22:8 and 16:14, were those obtained with 100% stoichiometric reductant addition. Considering that the valuable commodities were also diluted, it appears that the grades of FeO and V_2O_5 deporting to the byproduct stream were lower in the slags with target CaO:MgO ratios of 22:8.

The basicities of the slags are also included in Table VI. The definition of basicity used in the current work is shown by Equation [4]. The evaluation of the activities of Al_2O_3 and TiO_2 for consideration in the basicity expression fall outside the scope of the current study. The basicities of the slags in the current test work and the plant slags were similar and stable, irrespective of dilution by alumina. It thus appears that the effect of the alumina dilution factor on the respective slag components was constant.

$$\text{Basicity} = (\%MgO + \%CaO)/\ \%SiO_2 \qquad [4]$$

Table VI. Chemical compositions of the slags (mass%)

Test	CaO: MgO	MgO	Al_2O_3	SiO_2	CaO	TiO_2	V_2O_5	Cr_2O_3	MnO	FeO	Total	Basicity
EHSV slag		14.1	18.0	16.2	14.1	35.6	0.90	0.20	0.40	1.00	100.5	1.7
1	22:8	5.28	33.5	15.0	17.1	26.4	1.04	0.22	0.40	2.59	101.5	1.5
2	22:8	5.34	35.8	15.0	17.9	26.5	0.26	0.10	0.32	1.21	102.4	1.5
3	22:8	5.41	31.6	13.2	16.1	23.5	0.51	0.13	0.26	14.1	104.9	1.6
4*	22:8	3.34	21.4	10.2	12.1	18.7	1.03	0.25	0.24	43.6	110.8	1.5
5	16:14	11.9	18.7	19.4	16.3	32.4	1.80	0.26	0.53	1.37	102.6	1.5
6	16:14	12.4	19.8	18.6	16.2	33.9	0.53	0.11	0.43	0.57	102.5	1.5
7	16:14	12.3	19.4	18.2	16.6	32.8	0.33	<0.07	0.30	4.63	104.4	1.6
8*	16:14	5.94	9.05	9.72	8.32	17.9	1.41	0.32	0.25	63.1	116.0	1.5

CoO, NiO, CuO, PbO < 0.05%: respective analyte concentrations below the detection limit
<0.07%: analyte concentration below the detection limit
*Reason for high total unknown

Mineralogical Analysis

The slags with target ratios of CaO:MgO of 22:8 and 16:14 (*i.e.* slags produced with 100% stoichiometric

reductant addition) that resulted in the best Fe and V recoveries to alloy were subjected to mineralogical characterization by SEM-EDS and XRD and the results compared to the EHSV titanomagnetite slag characteristics. The phase chemical composition of the EHSV slag is shown in Figure 8 (Goso *et al*., 2015). The microstructure of the EHSV slag suggests that either pseudobrookite ($MgTi_2O_5$-Al_2TiO_5) or spinel [$(Mg)(Al,Ti)O_4$] could have crystallized as the primary phase. The perovskite content in the EHSV slag appears to be low. However, the microstructure of the laboratory-scale slag that was produced with a target CaO:MgO ratio of 16:14 and 100% stoichiometric reductant addition (Figure 9) shows that pseudobrookite is the primary phase. The large spinel phase contained pseudobrookite inclusions, suggesting that the pseudobrookite crystallized first and the spinel crystallized around it. A ternary phase in the form of perovskite is also observed.

The microstructure of the titanomagnetite slag with a target CaO:MgO ratio of 22:8 and 100% stoichiometric reductant addition is shown in Figure 10. The results show that perovskite ($CaTiO_3$), pseudobrookite, and spinel are the prevalent phases in the slag and occur as small crystals. It is not clear which of the three phases is primary. However, the prevalence of perovskite and pseudobrookite suggests that most of the titanium is in these phases, presenting an opportunity for titania to be extracted from the titanomagnetite slag. Titania is typically recovered from ilmenite slags with pseudobrookite as a major phase (van Dyk, 1999). Titania is also recoverable from perovskite by a salt roast and double water-acid leach process (Wang *et al*., 2010).

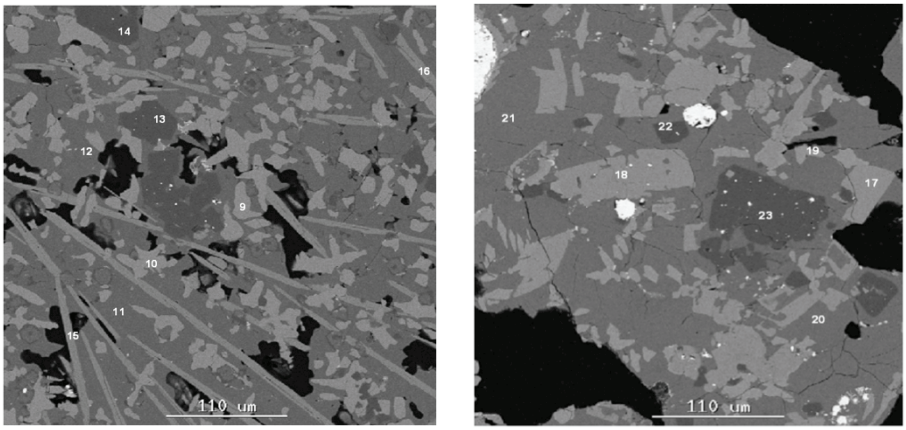

	MgO	Al_2O_3	SiO_2	CaO	TiO_2	V_2O_5	FeO	Phases
9	0.2	0.4	0.0	39.7	55.3	0.3	0.0	Perovskite
10	0.1	0.2	0.1	39.6	55.8	0.1	0.0	Perovskite
11	18.0	11.3	30.5	18.5	15.3	0.3	0.3	-
12	13.9	8.2	38.7	22.1	12.6	0.1	0.2	-
13	28.9	60.6	0.1	0.0	11.3	1.7	0.3	Spinel
14	28.9	63.0	0.2	0.1	8.0	2.3	0.2	Spinel
15	9.4	2.0	0.7	1.0	81.6	0.3	0.6	Pseudobrookite
16	8.9	2.1	0.3	0.7	82.3	1.1	0.2	Pseudobrookite
17	5.8	2.7	0.1	0.2	90.3	0.2	0.1	Pseudobrookite
18	9.3	1.8	0.3	0.3	86.6	1.9	0.0	Pseudobrookite
19	0.2	0.3	0.1	39.5	56.1	0.0	0.1	Perovskite
20	10.5	9.7	34.8	23.4	16.7	0.1	0.2	-
21	9.6	10.1	34.3	23.9	18.6	0.4	0.2	-
22	28.1	65.2	0.3	0.1	7.9	0.7	0.4	Spinel
23	27.6	62.5	0.5	0.2	9.2	1.4	0.4	Spinel

- Not detected by XRD

Figure 6. Typical backscattered electron images and EDS analysis (mass%) of a titanomagnetite slag produced by EHSV (Goso *et al*., 2015)

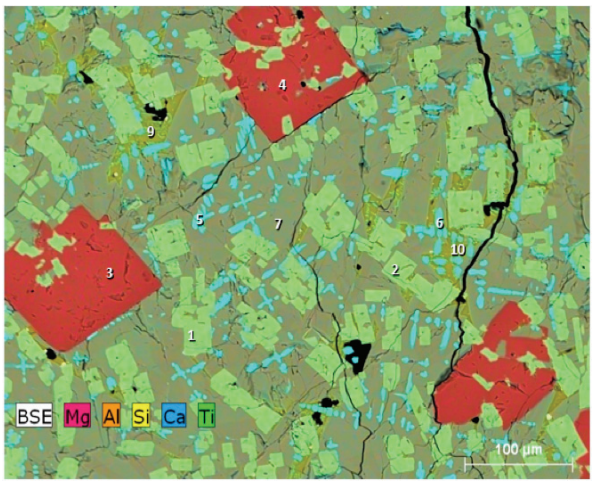

	MgO	Al_2O_3	SiO_2	CaO	TiO_2	V_2O_5	MnO	FeO	Phases
1	8.0	5.9			80.8	5.3			Pseudobrookite
2	7.6	5.8			81.3	5.2			Pseudobrookite
3	28.1	60.1			6.7	4.6		0.6	Spinel
4	25.7	58.9			8.3	5.9	0.4	0.9	Spinel
5				38.8	61.2				Perovskite
6				41.2	58.8				Perovskite
7	11.4	17.7	30.3	24.2	15.8			0.7	-
8	10.8	15.5	31.4	24.7	14.6		1.4	1.5	-
9	1.4	23.0	42.2	10.2	4.0		6.6	5.5	-
10	1.1	23.7	47.4	8.1	1.8		6.7	4.8	-

- Not determined by XRD

Figure 7. Backscattered electron image and EDS analysis (mass%) and XRD phase identification in titanomagnetite slag with target CaO:MgO ratio of 16:14 produced with 100% stoichiometric reductant addition

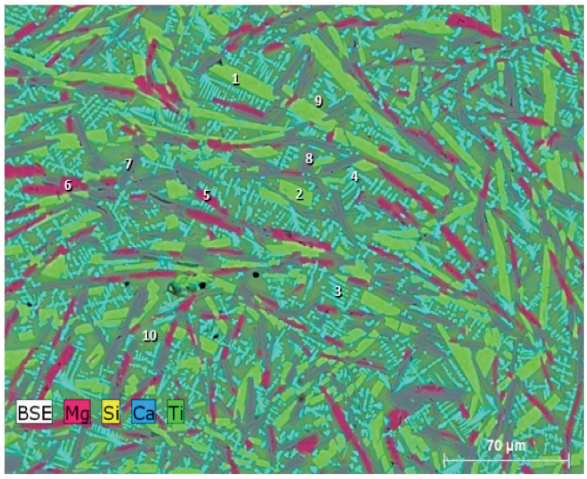

	MgO	Al_2O_3	SiO_2	CaO	TiO_2	FeO	Phases
1	3.0	7.5		0.90	88.6		Pseudobrookite
2	4.3	9.8		0.60	85.3		Pseudobrookite
3		4.3	3.9	38.0	53.8		Perovskite
4		5.1	6.0	37.4	51.4		Perovskite
5	25.6	65.8			5.3	2.2	Spinel
6	24.5	66.8			4.4	2.6	Spinel
7	5.1	69.2		9.2	16.4		
8	6.2	64.6		9.6	19.7		
9	3.2	28.5	34.7	24.2	7.1	1.1	
10	3.6	27.3	35.8	25.7	5.6	0.8	

- Not determined by XRD

Figure 8. Backscattered electron image and EDS analysis (mass%) and XRD phase identifications in titanomagnetite slag with target CaO:MgO ratio of 22:8 produced with 100% stoichiometric reductant addition.

CONCLUSIONS AND RECOMMENDATIONS

The test results demonstrated that the Fe and V recoveries to the alloy phase are similar in both slag systems. However, in the titanomagnetite slag with a target CaO:MgO ratio of 22:8 the titania is concentrated mainly in the perovskite and pseudobrookite phases. The spinel content in this slag appears to be low. Hence, this slag presents an opportunity for further beneficiation to recover titanium, which is currently not undertaken. The prospective increase in the scope of the products generated from titanomagnetite would result in the intensification of the primary titanomagnetite process economics and maximize the exploitation of the valuable titanomagnetite deposits of the Bushveld Complex and other African deposits, including the Tete deposit in Mozambique. These results constitute a significant milestone towards the development of efficient titanomagnetite smelting technologies for the development and sustainability of the South African, and even the entire African, minerals industry.

ACKNOWLEDGMENTS

The authors thank A. Corfield for assistance with mineralogical characterization, and the Analytical Services Division of Mintek for assistance with chemical analysis. The financial support of Mintek is greatly appreciated.

REFERENCES

Fischer, R. P. (1975). Vanadium resources of titaniferous magnetite deposits. *GEOLOGY AND RESOURCES OF VANADIUM DEPOSITS, 926-B*, B1-B10.

Bleloch, W. (1949). The electric smelting of iron ores for production of alloy irons and steels and recovery of chromium and vanadium. *Journal of the chemical metallurgical and mining society of South Africa, 49*, 363-408.

Rohrmann, B. (1985). Vanadium in South Africa. *Journal of the South African Institute of Mining and Metallurgy, 85*(5), 141 -150.

Anderson. (2013, 07 08). *Mining*. (BusinessDay) Retrieved 10 05, 2016, from www.bdlive.co.za: http://www.bdlive.co.za/business/mining/2013/07/08/nyanza-eyes-beneficiation-with-a-r4.2bn-plant

Steinberg, W. S. (2008, December). *dspace*. Retrieved 10 10, 2016, from www.repository.up.ac.za: http://repository.up.ac.za/bitstream/handle/2263/26090/dissertation.pdf;sequence=1

Goso, X. C., Nell, J., & Petersen, J. (2015). Review of liquidus surface and phase equilibria in the TiO2-SiO2-Al2O3-MgO-CaO slag system at pO2 applicable in fluxed titaniferous magnetite smelting. *Conference on Molten Slags, Fluxes and Salts (MOLTEN16)* (pp. 105-114). Seattle: The Minerals, Metals and Materials Society.

Jochens, P. R., Sommer, G., & Howat, D. D. (1969). Preliminary equilibrium and non-equilibrium phase studies of titaniferous slags. *Journal of The Iron and Steel Institute*, 187-192.

Zhang, L., Zhang, L. N., Wang, M. Y., Li, G. Q., & Sui, Z. T. (2007). Recovery of titanium compounds from molten Ti-bearing blast furnace slag under the dynamic oxidation condition. *Minerals Engineering, 20*, 684–693.

Steinberg, W. S., Geyser, W., & Nell, J. (2011, 03 6-9). The history and devleopment of the pyrometallurgical processes at Evraz highveld Steel and Vanadium. *Southern African Pyrometallurgy* (pp. 63-76). Johannesburg: South African Institute of Mining and Metallurgy. Retrieved 10 10, 2016, from www.saimm.co.za: http://www.saimm.co.za/Conferences/Pyro2011/

Van Dyk, J. P. (1999, November 05). *Theses and Dissertations (University of Pretoria)*. Retrieved 10 10, 2016, from www.dspace.up.ac.za: http://www.dspace.up.ac.za/handle/2263/28654?show=full

Wang, Y., Qi, T., Chu, J., & Zhao, W. (2010). Production of TiO2 from CaTiO3 by alkaline roasting method. *RARE METALS, 29*(2), 162-167.

Martin Bongani Sitefane

Mintek
Technician

Started working at Mintek as an in-service trainee in order to fulfil of the National Diploma requirements in 2014. Thereafter, Mintek recruited me in 2015 whilst still studying towards a Btech in Extraction Metallurgy at the University of Johannesburg. Completed the B-tech in the same year and I am now studying towards a BSc honours at the University of Pretoria. Work experience includes both laboratory and pilot scale exposure in smelting of: ilmenite, iron ore, PGM, manganese, chromite etc. Other exposed areas include converting of PGM and pig iron, pre-reduction and roasting of various ores.